Supplementary Material
Resolving Decades of Debate: The Surprising Role of High-Temperature Covalency in the Structure of Liquid Gallium

Stephanie Lambie[1], Krista G. Steenbergen[2], and Nicola Gaston[1]

[1] *MacDiarmid Institute for Advanced Materials and Nanotechnology, Department of Physics, University of Auckland, Private Bag 92019, Auckland, New Zealand*
[2] *MacDiarmid Institute for Advanced Materials and Nanotechnology, School of Chemical and Physical Sciences, Victoria University of Wellington, P.O. Box 600, Wellington 6140, New Zealand*

May 13, 2024

1 Computational details

Ab initio molecular dynamics (AIMD) simulations are carried out using the Vienna *ab initio* Simulation Package (VASP).[1] The Perdew-Becke-Ernzerhof for solids (PBEsol)[2] exchange correlation functional was used in conjunction with the projector augmented wave (PAW) method.[3] An energetic cut off of 350 eV and Γ-centred k-points were used for all AIMD simulations. For equilibration AIMD simulations, the isobaric-isothermal (nP_zT) ensemble employing the Langevin thermostat and Parinello-Rahman method[4,5] was used, while for production AIMD simulations the canonical (nVT) ensemble with the Nosé-Hoover thermostat[6–8] was utilised.

Bulk liquid Ga calculations were carried out at three temperatures; 320 K, 450 K and 1000 K. Supercells were created for each temperature simulation; for the 320 K simulation, the 8-atom α-Ga unit cell was repeated by 4×2×6 to create a 384 atom supercell while for the 450 K and 1000 K simulations, the α-Ga unit cell was repeated by 4×2×3 to provide a 192 atom supercell. Due to its proximity to the solidification temperature, the 320 K supercell needed to be doubled to allow the low-temperature liquid phase to be stabilised.

The supercells were shocked to 3000 K using a timestep of 4 fs for a period of 4 ps to ensure the simulations were fully liquid. For the 320 K simulation, the 3000 K liquid was equilibrated at 450 K before being quenched to 320 K using a timestep of 2 fs and a cooling rate of 0.1 K fs^{-1}. For the 1000 K and 450 K simulations, the liquidated structures were equilibrated at each temperature, respectively. Initial liquid structures are shown in Figure 1.

All three simulations were equilibrated at their designated temperature by carrying out short equilibration runs of 200 timesteps and timestep of 4 fs until the pressure in the xy dimension was ±10 kB throughout the run. Between the equilibration runs, the x and y lattice dimensions were altered manually to reduce the pressure on the unit cell as only the z-lattice dimension barostats within the nP_zT ensemble. Once the pressure was sufficiently low, production runs were carried out using a timestep of 4 fs for a total duration of 104 ps; pressures were monitored throughout the simulation are shown in Figure 2.

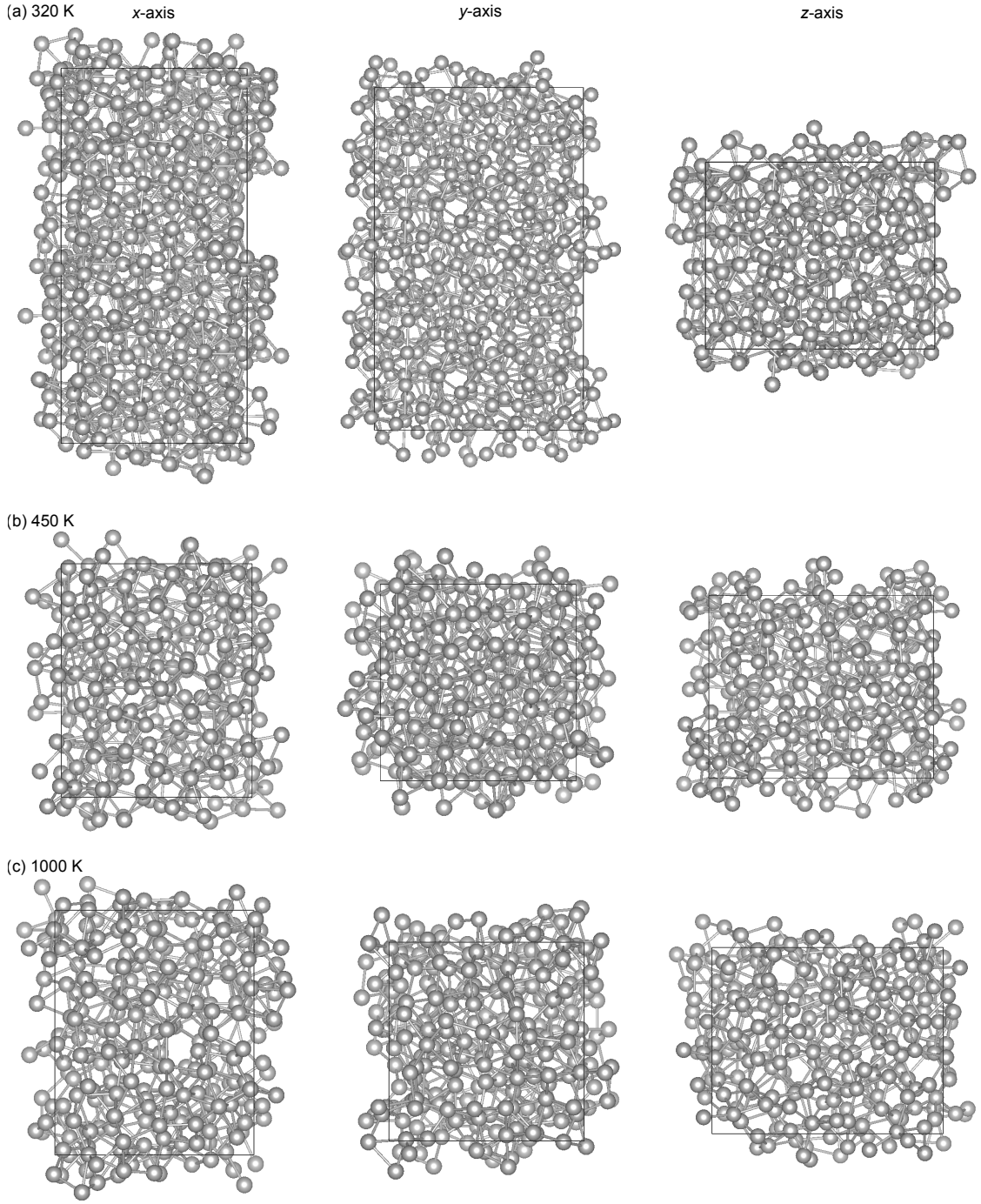

Figure 1: Initial structures for the *(a)* 320 K, *(b)* 450 K and *(c)* 1000 K simulations. The left column shows the view down the x-axis, the centre column shows the view down the y-axis and the right column shows the view down the z-axis.

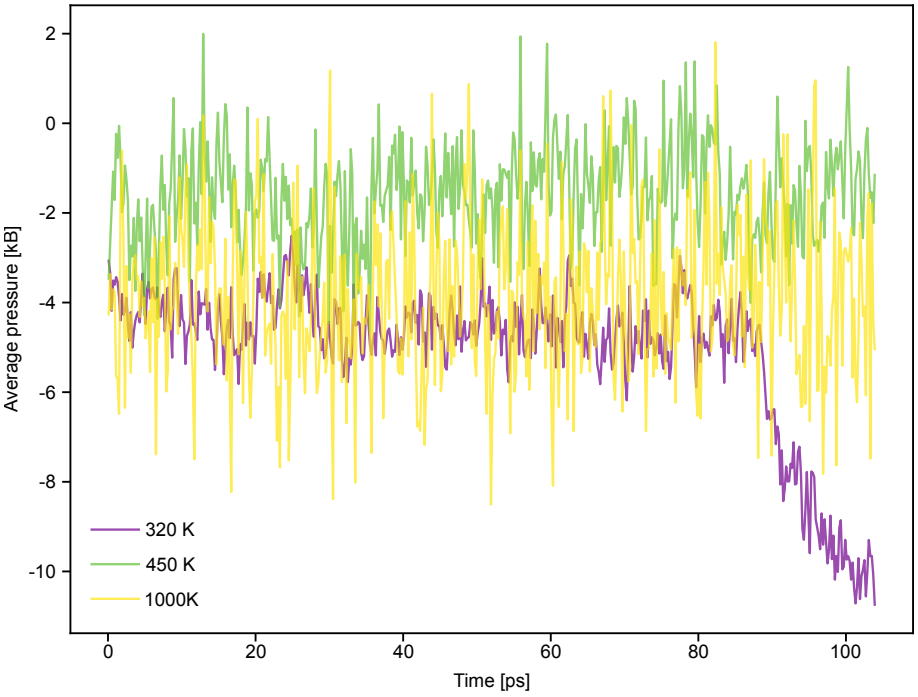

Figure 2: Total pressures on the unit cell throughout the simulation for 320 K (purple), 450 K (green) and 1000 K (yellow). Pressures are averaged over 50 timesteps to reduce the noise in the data. The negative pressure that is observed in the 320 K simulation from ∼80 ps corresponds to a phase change to the solid. Note: only data from 40-64 ps was used to determine covalency in the liquid systems throughout the main text.

2 Structure factor

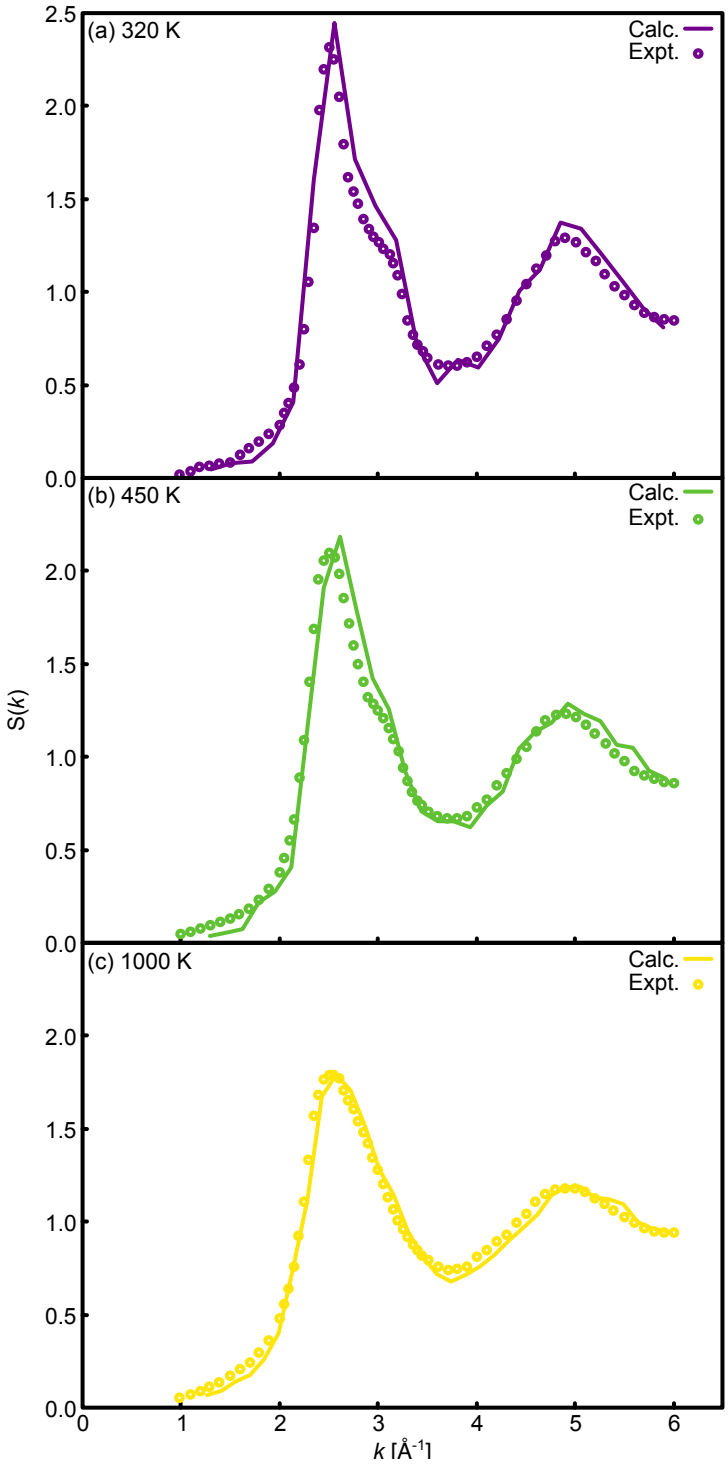

Figure 3: Comparison of the S(k) calculated at *(a)* 320 K, *(b)* 450 K and *(c)* 1000 K compared to the experimental results of Waseda *et al.*[9] measured at 323 K, 473 K and 1073 K, respectively.

3 Radial distribution function analysis

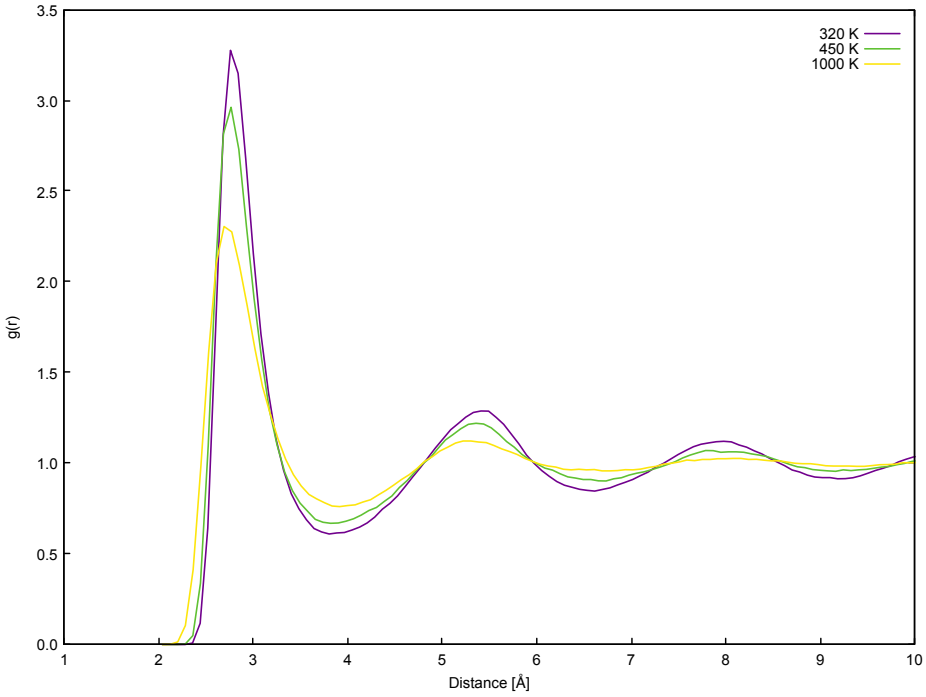

Figure 4: Radial distribution function analysis calculated between 40 and 64 ps for the 320 K (purple), 450 K (green) and 1000 K (yellow) Ga liquid.

4 Angular distribution function analysis

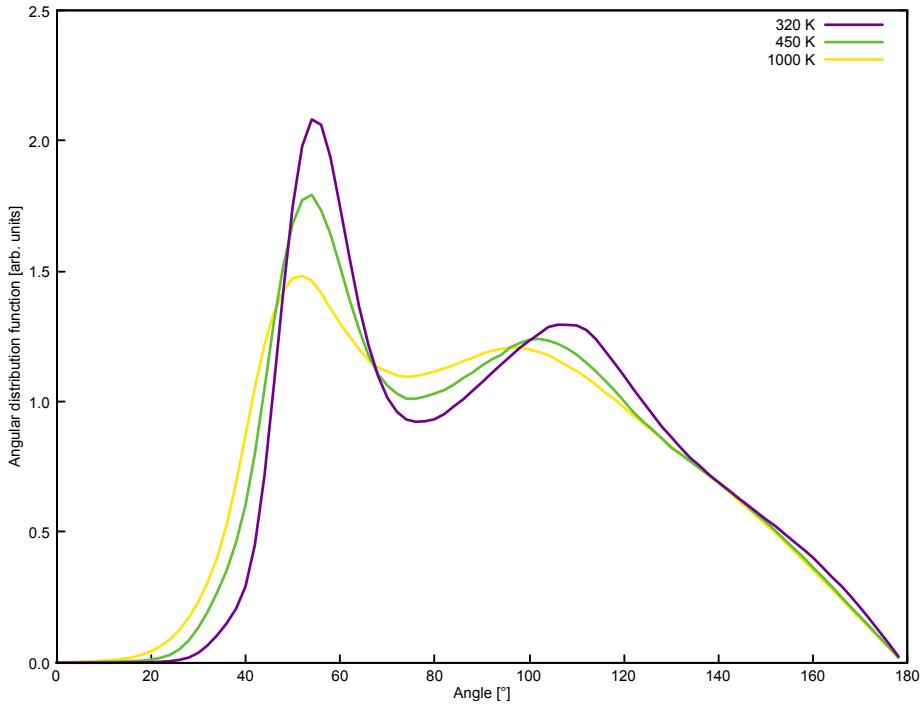

Figure 5: Angular distribution function analysis calculated between 40 and 64 ps for the 320 K (purple), 450 K (green) and 1000 K (yellow) Ga liquid.

5 Mean square displacement analysis

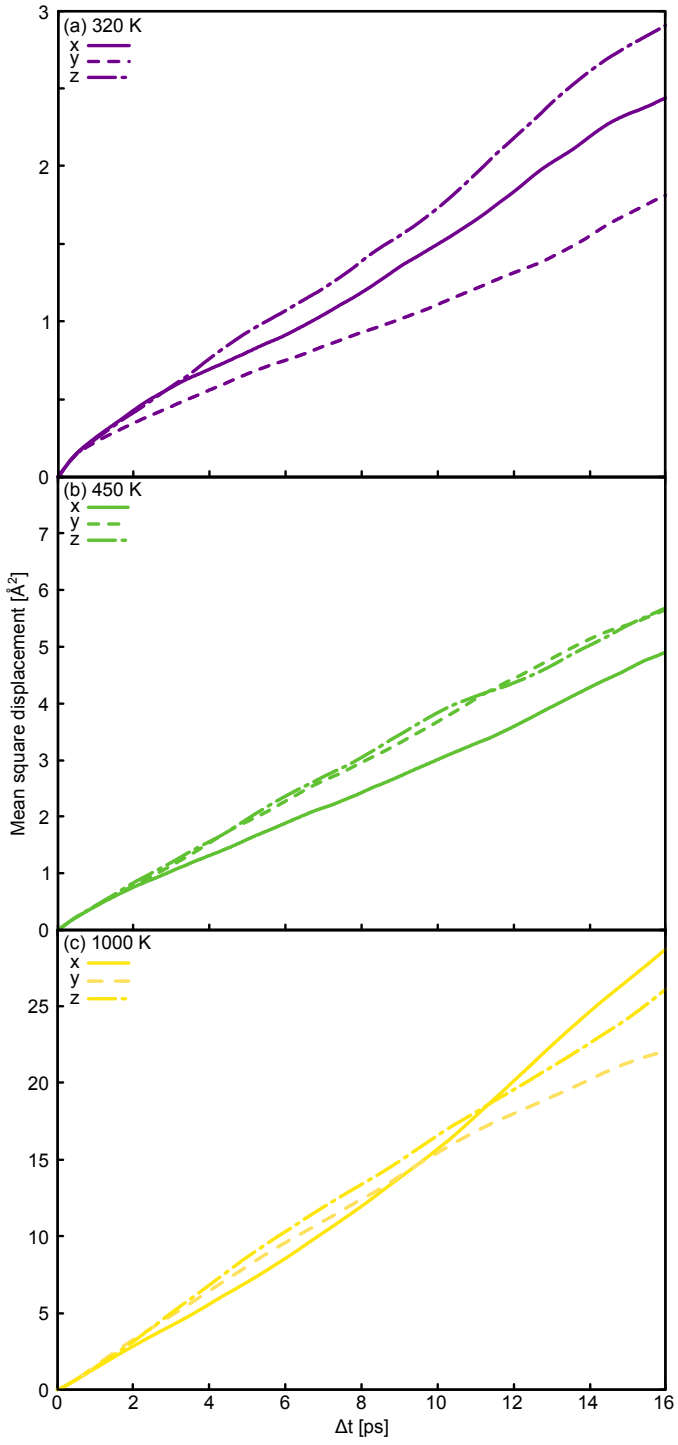

Figure 6: Mean square displacement analyses calculated between 40-64 ps at *(a)* 320 K, *(b)*450 K and *(c)* 1000 K. Note: different scales of the y-axes between temperatures are used.

6 First nearest neighbour distances

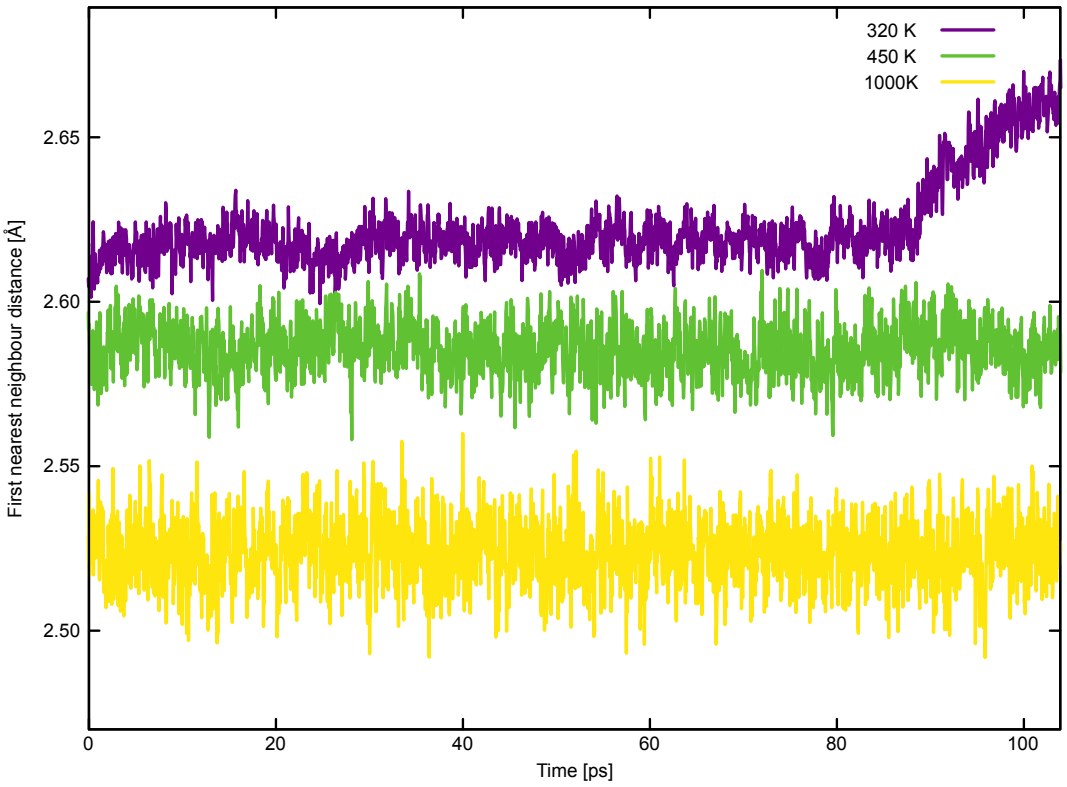

Figure 7: Average first nearest neighbour distances for the 320 K (purple), 450 K (green) and 1000 K (yellow) Ga liquid. Note: The increase in first nearest neighbour distance within the 320 K simulation resulted from our simulation freezing. To ensure all results are presented from fully liquid simulations, we have only presented data from the 40-64 ps simulation range.

7 Steinhardt order parameters

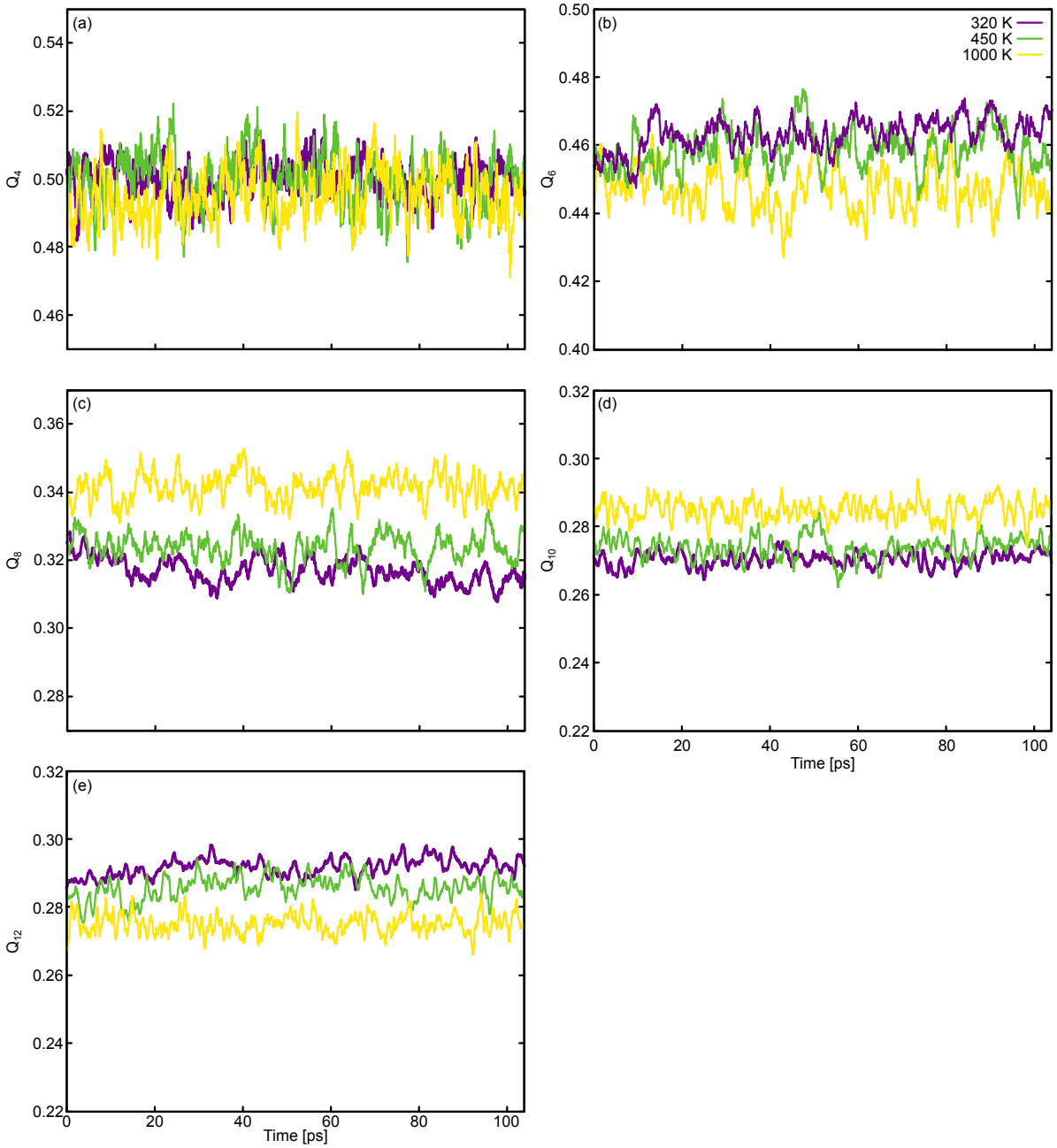

Figure 8: Steinhardt order parameters calculating using *(a)* four, *(b)* six, *(c)* eight, *(d)* ten and *(e)* twelve nearest neighbours. Order parameters calculated at 320 K are shown in purple, 450 K in green and 1000 K in yellow.

8 Isosurface value test

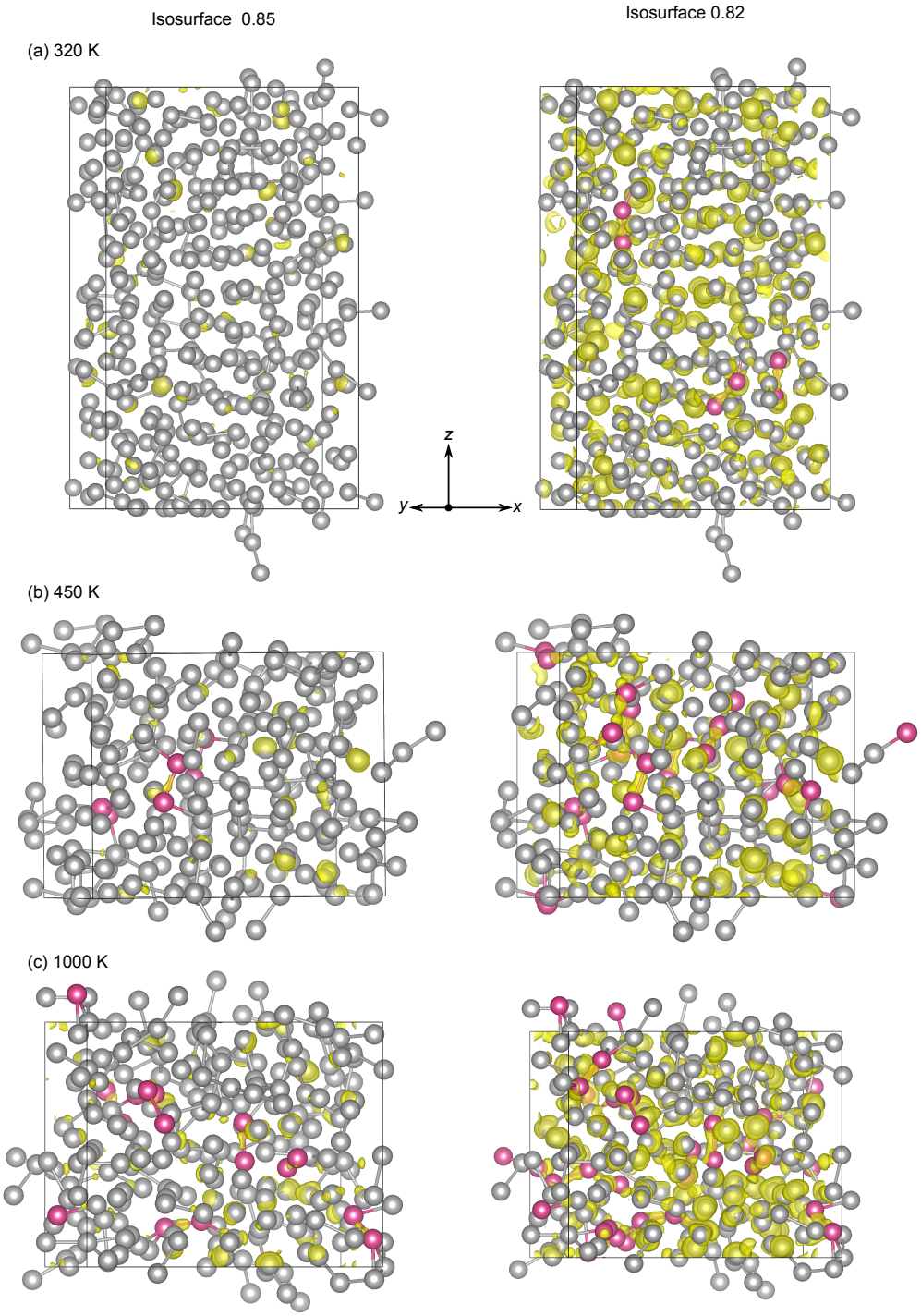

Figure 9: Effect of lowering the isosurface value from 0.85 to 0.82 for the 16 ps snapshots at each temperature, as an example. We note the 0.82 isosurface value is still obnoxiously high, compared to the usual isosurface value of 0.60 used to diagnose covalency. Ga atoms involved in metallic bonding are shown in grey while Ga atoms involved in a covalent bond are shown in red.

Table 1: Percentage of atoms involved in a covalent bond for each temperature at 0.85 and 0.82 isosurface using the 16 ps snapshot from Figure 9 as an example.

Temperature [K]	% of the atoms involved in a covalent bond	
	Isosurface 0.85	Isosurface 0.82
320	0.00	1.56
450	3.13	9.18
1000	6.25	14.80

We determine that using such harsh criteria for determining covalency within the liquid makes our conclusions on the degree of covalency within the liquid conservative. Furthermore, we do not include covalent interactions that extend through the periodic boundary, which is another way in which we are undercounting the degree of covalency within the liquid, thus making our conclusions conservative.

9 Bader atoms-in-molecule analysis

Bader charge analyses[10,11] were also carried out on selected electron localisation function (ELF) snapshots by requesting output of the AECCAR files from VASP. After subtracting the core charge to obtain the valence-only Bader charges, this analysis found either one or two pools of charge that total between 1.8 e and 2.5 e exactly on the bond axis (177° or greater) between two Ga atoms for every covalent bond identified in the ELF analysis. Counter-cases, whereby the ELF did not identify a covalent bond, were also analysed using the Bader analysis and here, charge pooling on the bond axis was not observed.

10 Electron localisation function analysis snapshots

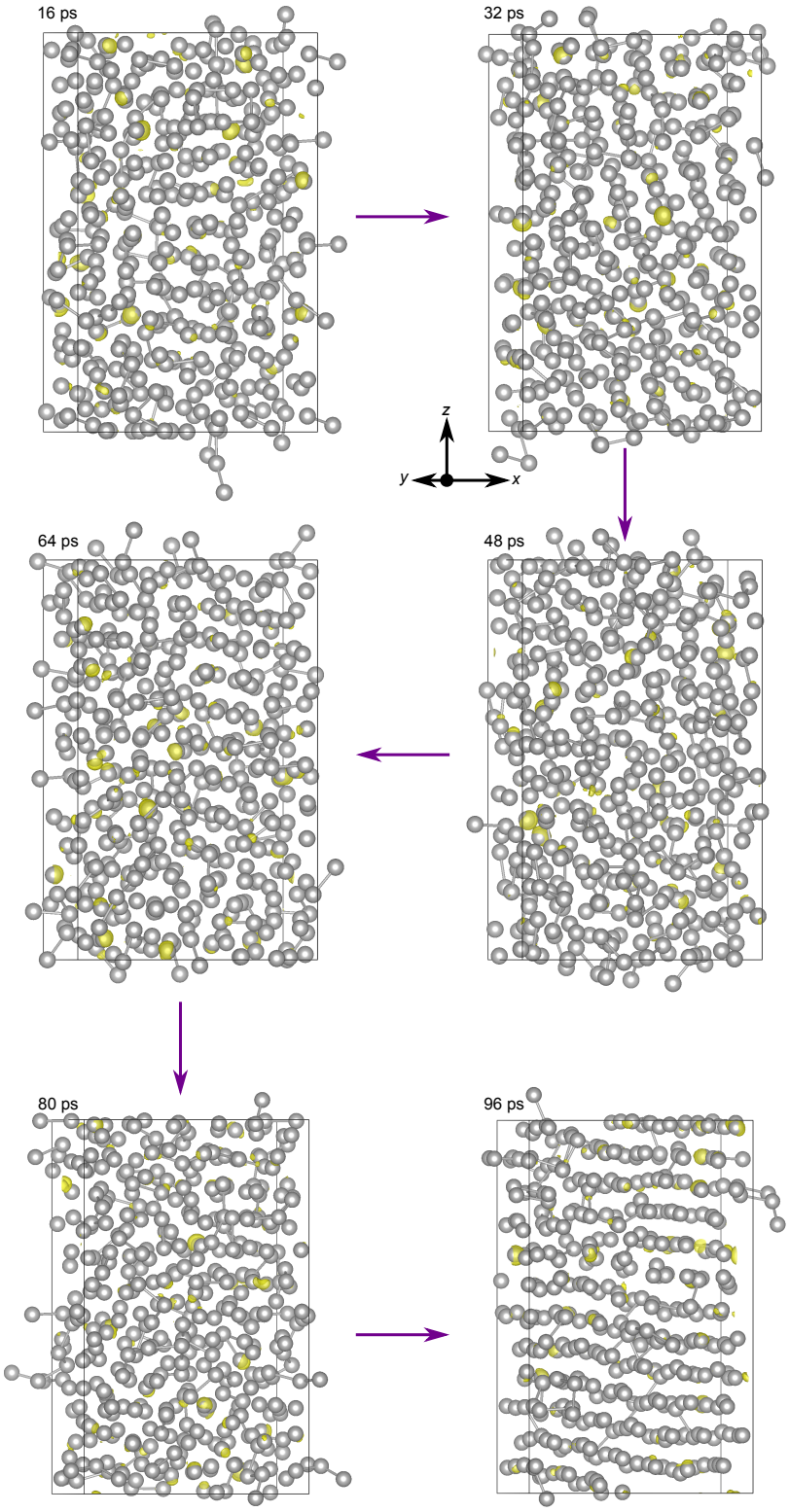

Figure 10: Snapshot electron localisation function (ELF) analyses for the 320 K liquid. Ga atoms involved in metallic bonding are shown in grey while Ga atoms involved in a covalent bond are shown in red. ELF isosurface value is set to 0.85 and bonds $\leq$ 2.6 Å are shown.

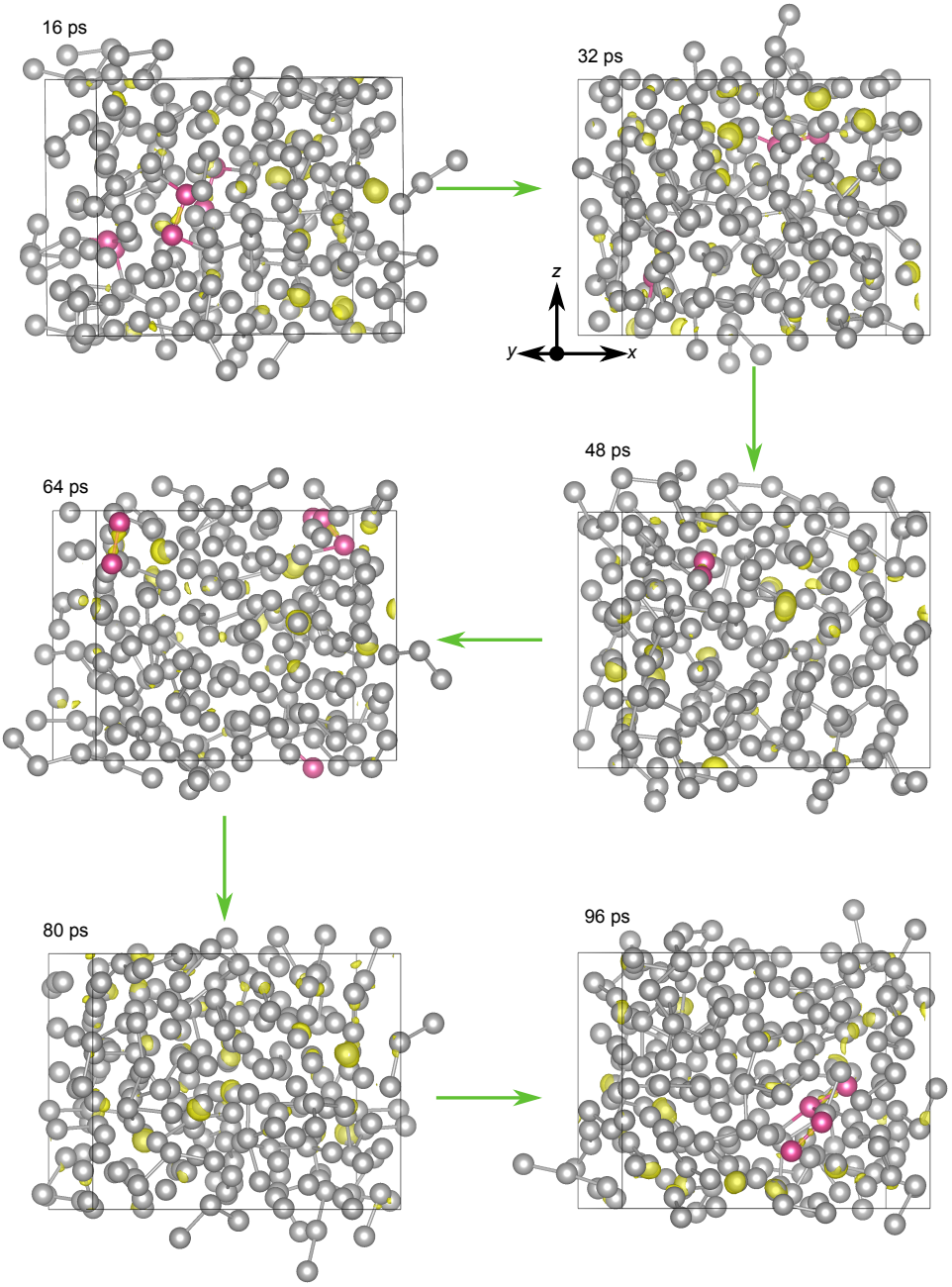

Figure 11: Snapshot electron localisation function (ELF) analyses for the 450 K liquid. Ga atoms involved in metallic bonding are shown in grey while Ga atoms involved in a covalent bond are shown in red. ELF isosurface value is set to 0.85 and bonds $\leq$ 2.6 Å are shown.

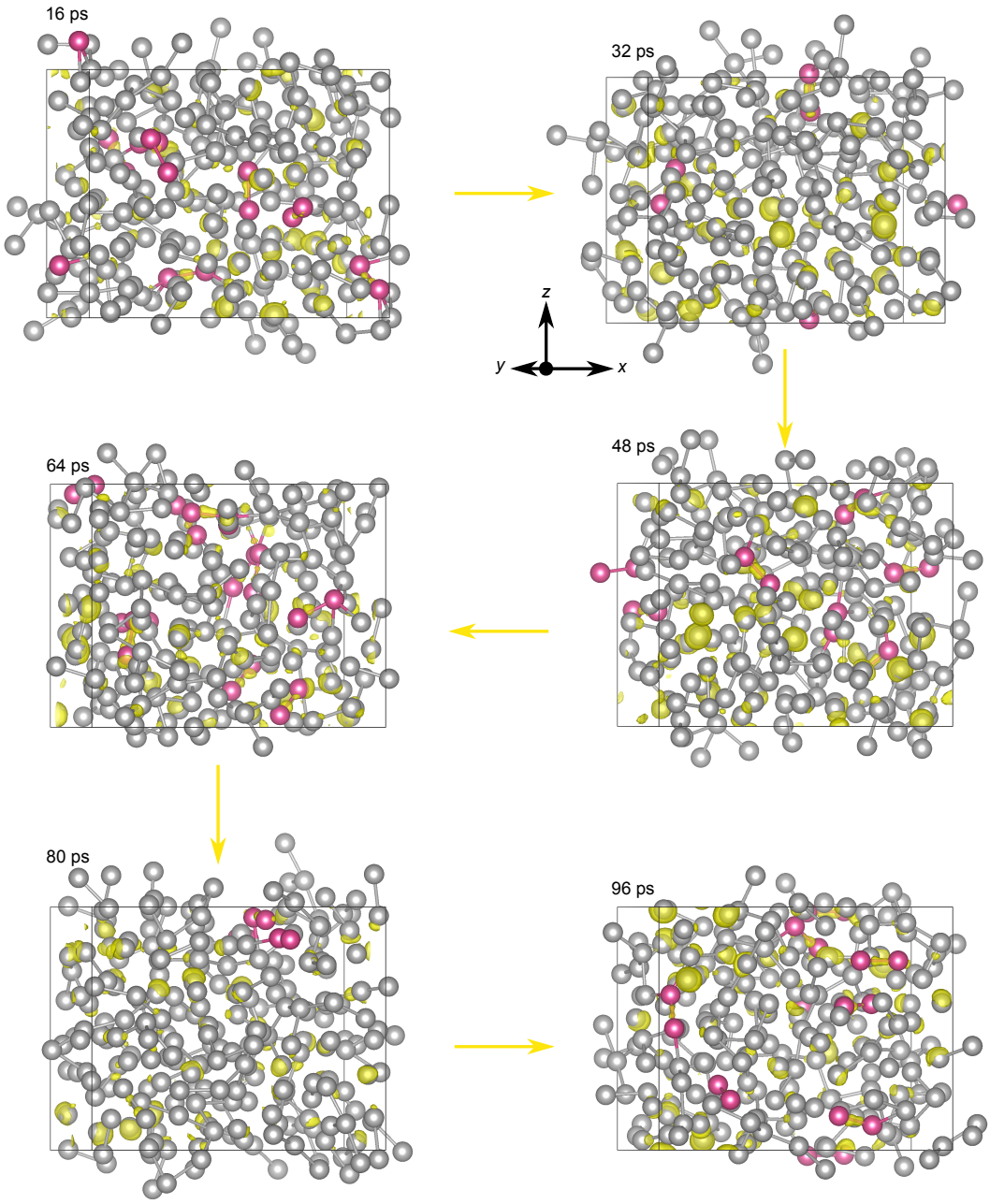

Figure 12: Snapshot electron localisation function (ELF) analyses for the 1000 K liquid. Ga atoms involved in metallic bonding are shown in grey while Ga atoms involved in a covalent bond are shown in red. ELF isosurface value is set to 0.85 and bonds $\leq$ 2.6 Å are shown.

11 Covalency definitions

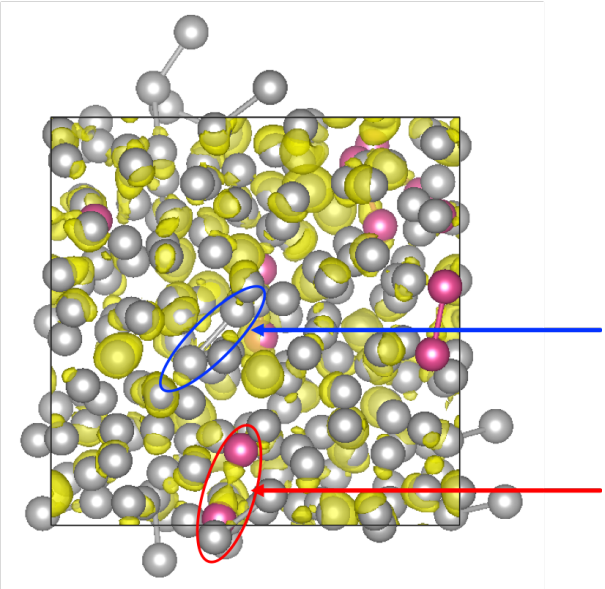

Figure 13: A electron localisation function analysis snapshot, with bonds less than 2.5 Å being drawn in, showing, in blue, that not all bonds less with 2.5 Å are covalent and, in red, that not all covalent bonds are less than 2.5 Å. Isosurface value set to 0.82.

12 Algorithm for calculating longevity of bonds

Here, we present our conservative algorithm for determining a proxy for the longevity of covalency within the liquid structures.

For each atom i, in a simulation, the analysis code calculates the first nearest neighbour distance. While the first nearest neighbour distance is less than 2.45 Å for longer than 4 timesteps (16 fs), the duration is calculated and considered to be the longevity of a covalent bond.

Assumptions of the algorithm

1. The algorithm assumes that covalency only exists for interactions that are less than 2.45 Å in length, which is not the case and therefore, some covalent interactions are being missed, which undercounts the covalent interactions, which have a longer lifetime, due to the electron localisation between two atoms, thus making our results conservative.

2. The algorithm assumes that all interactions of less than 2.45 Å are covalent in nature, and therefore, by using a cut-off, we are over-counting metallic interactions which we expect have a shorter lifetime than covalent interactions due to the lack of electron localisation between atoms thus making our results conservative.

3. The algorithm assumes that the first nearest neighbour interaction is the interaction most likely to be of a covalent nature, which does not necessarily have to be the case.

13 Consecutive timestep electron localisation function analysis

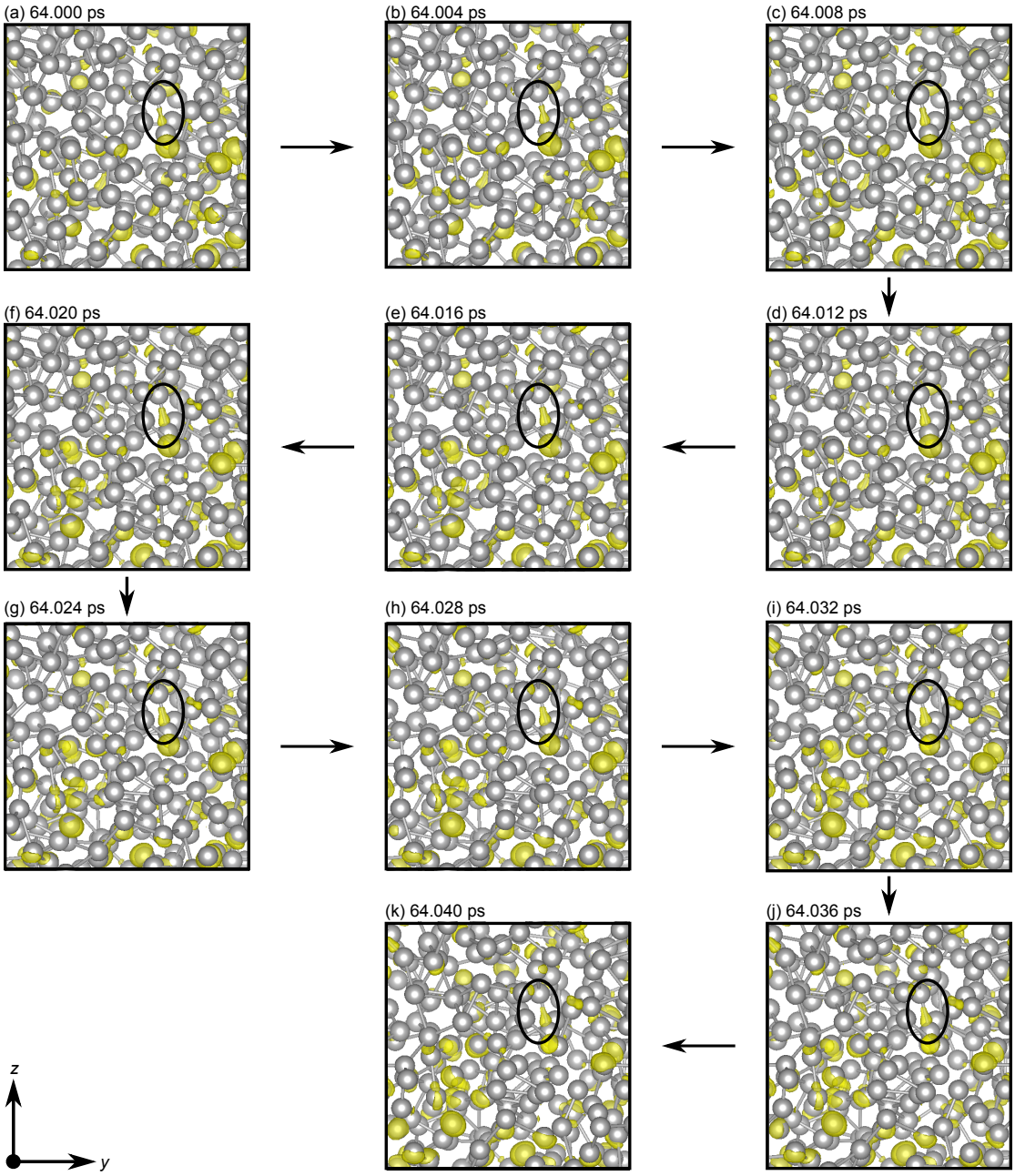

Figure 14: Electron localisation function analysis carried out over 11 consecutive timesteps for the 1000 K liquid from 64.000 ps (16000 timesteps) to 64.040 ps (16010 timesteps). In each snapshot, a covalent bond is highlighted that is persistent throughout the consecutive snapshots which highlights that these localised regions of electron density can be persistent over time. Isosurface value is set to 0.85 and bonds $\leq$ 2.7 Å are shown.

14 Velocity autocorrelation function

14.1 Velocity data

VASP does not store velocities every timestep. Numerical velocities are therefore obtained by taking the forward finite difference of the position data (which was stored at every AIMD timestep). Velocities obtained in this way will differ slightly from those obtained internally by VASP by the velocity Verlet algorithm; however, due to the small timestep chosen, the differences will be negligible.

14.2 Calculation of the velocity autocorrelation function

The velocity autocorrelation function (VACF) quantifies the correlation of the velocity of an atom with itself some time τ later. It is defined as:

$$C(\tau) = \langle \vec{v}(t) \cdot \vec{v}(t+\tau) \rangle \ , \tag{1}$$

where $\vec{v}(t)$ is the velocity of an atom at time t and τ is the time lag.

The VACF was calculated for the three simulation temperatures for the simulation range 40-64 ps (6000 frames). The VACF is an average quantity taken over all atoms and all time origins, as:

$$C(\tau_m) = \frac{1}{N}\frac{1}{n_{TO}} \sum_{j=0}^{N-1} \sum_{\ell=0}^{n_{TO}-1} \vec{v_j}(t_\ell) \cdot \vec{v_j}(t_\ell + \tau_m) \ , \tag{2}$$

where N is the number of atoms, n_{TO} is the number of time origins, and $\vec{v_j}(t_\ell)$ is the velocity of atom j at time origin ℓ. The time lag, τ_m, is calculated from $\tau = 0$ to some upper bound $\tau_{\max}$, which we set to 1500 timesteps (6 ps).

Note: The VACF is typically normalised by C($\tau = 0$). However, in order to be able to compare the magnitude of the velocity correlations (and, in particular, the subsequent power spectrum results) between the different simulation temperatures, we leave the VACF *unnormalised*. Figure 15 shows the unnormalised VACF computed for each of the three temperatures.

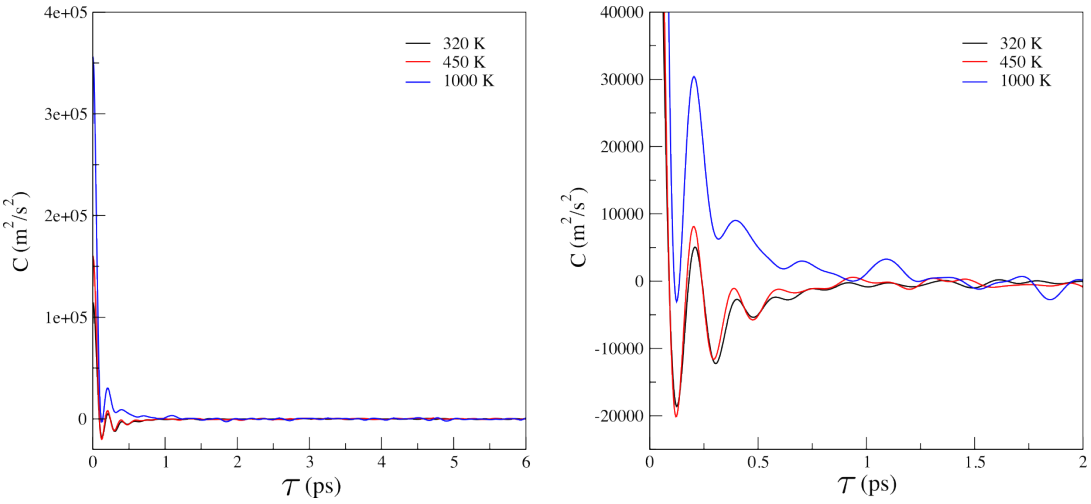

Figure 15: Unnormalised velocity autocorrelation function (VACF) for three different temperatures. The right plot is simply a replica of the left, with a reduced range for both VACF and τ, to show more detail.

Power spectrum of the VACF

In order to investigate frequency modes, we take the discrete Fourier transform of the VACF as

$$\hat{C}(f_k) = \sum_{m=0}^{M-1} [\, C(\tau_m) w(\tau_m) \,]\, e^{-i2\pi f_k \tau_m} \tag{3}$$

where f_k is the frequency and $w(\tau_m)$ is the Hamming window (applied in order to reduce spectral leakage) given by

$$w(\tau_m) = 0.54 - 0.46 \cos\left(\frac{2\pi\tau_m}{T}\right) . \tag{4}$$

Here, the period T is taken to be the full range over which the VACF is calculated (zero to $\tau_{\max}$). The power spectrum is then obtained by squaring the coefficients of the Fourier transform.

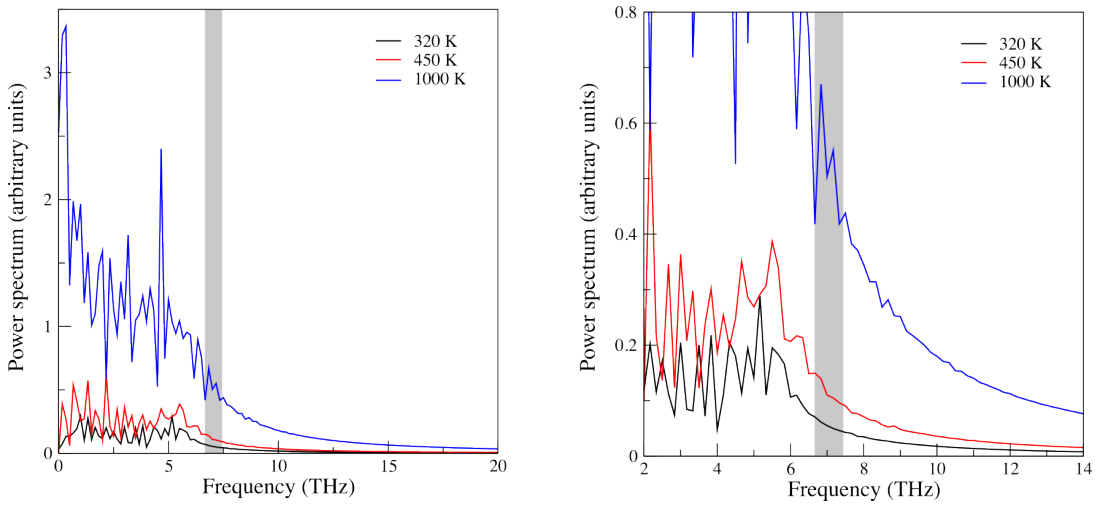

Figure 16: Power spectrum of the (unnormalised) velocity autocorrelation function, $C(\tau)$, for the three simulation temperatures. The right plot is simply a replica of the left, with a reduced range for both frequency and power spectrum, in order to show more detail. The grey box in both plots indicates the frequency range over which the covalent stretching modes are typically observed.

Fig. 16 gives the power spectrum for each of the three simulation temperatures. Several theoretical and experimental studies suggest that the covalent bond stretching modes in α-Ga range from 6.7-7.4 THz.[12–15] Focussing on this range in the power spectrum (Fig. 16), we find clear evidence of increasing covalent vibrational signatures. The 450 K power spectrum has a distinct shoulder in this range, while the 1000 K simulation has two clear peaks. However, the 320 K power spectrum is smoothly decreasing in that frequency range. This correlates perfectly with the increasing covalent nature of the gallium liquid with increasing temperature.

References

[1] Kresse, G., Furthmüller, J. Efficient iterative schemes for ab initio total-energy calculations using a plane-wave basis set. *Phys. Rev. B* **1996**, *54*, 11169.

[2] Perdew, J., Ruzsinszky, A., Csonka, G., Vydrov, O., Scuseria, G., Constantin, L., Zhou, X., Burke, K. Restoring the density-gradient expansion for exchange in solids and surfaces. *Phys. Rev. Lett.* **2008**, *100*, 136406.

[3] Blöchl, P. Projector augmented-wave method. *Phys. Rev. B* **1994**, *50*, 17953–17979.

[4] Parrinello, M., Rahman, A. Polymorphic transitions in single crystals: A new molecular dynamics method. *J. Appl. Phys.* **1981**, *52*, 7182–7190.

[5] Parrinello, M., Rahman, A. Crystal structure and pair potentials: A molecular-dynamics study. *Phys. Rev. Lett.* **1980**, *45*, 1196–1199.

[6] Nosé, S. A unified formulation of the constant temperature molecular dynamics methods. *J. Chem. Phys.* **1984**, *81*, 511–519.

[7] Nosé, S. A molecular dynamics method for simulations in the canonical ensemble. *Mol. Phys.* **1984**, *52*, 255–268.

[8] Hoover, W. Canonical dynamics: Equilibrium phase-space distributions. *Phys. Rev. A* **1985**, *31*, 1695–1697.

[9] Waseda, Y. *The structure of non-crystalline materials: liquids and amorphous solids*; McGraw-Hill Publishing: New York, 1980.

[10] Bader, R. F. W. A quantum theory of molecular structure and its applications. *Chem. Rev.* **1991**, *91*, 893–928.

[11] Henkelman, G., Arnaldsson, A., Jónsson, H. A fast and robust algorithm for Bader decomposition of charge density. *Comp. Mater. Sci.* **2006**, *36*, 354–360.

[12] Remsing, R., Sun, J., Waghmare, U., Klein, M. Bonding in the metallic molecular solid α-gallium. *Mol. Phys.* **2018**, *116*, 3372–3379.

[13] Creighton, J. A., Withnall, R. The Raman spectrum of gallium metal. *Chem. Phys. Lett.* **2000**, *326*, 311–313.

[14] Quan, Y., Hirschfeld, P. J., Hennig, R. G First-principles study of superconductivity in α and β gallium. *Phys. Rev. B* **2021**, *104*, 075117.

[15] Spagnolatti, I., Bernasconi, M. *Ab initio* phonon dispersion relations of α-Ga. *Eur. Phys. J. B* **2003**, *36*, 87–90.